AD-A254 401

ΓATION PAGE

je 1 hour per response, including the time for reviewing instructions, searching existing data sources, gathering and mation. Send comments regarding this burden or any other aspect of this collection of information, including suggestions r Information Operations and Reports, 1215 Jefferson Davis Highway, Suite 1204, Arlington, VA 22202-4302, and to 188), Washington, DC 20503.

	›. August 1992	**3. Report Type and Dates Covered.** Final - Journal Article

4. Title and Subtitle. The Fall Rate of the T-7 XBT	**5. Funding Numbers.**

DTIC
ELECTE
AUG 2 5 1992
S C D

6. Author(s). Zachariah R. Hallock and William J. Teague	

Contract

Program Element No.	0604704N
Project No.	R1740
Task No.	300
Accession No.	DN259042
Work Unit No.	13311M

7. Performing Organization Name(s) and Address(es). Naval Oceanographic and Atmospheric Research Laboratory Ocean Science Directorate Stennis Space Center, MS 39529-5004	**8. Performing Organization Report Number.** JA 331:042:91

9. Sponsoring/Monitoring Agency Name(s) and Address(es). Naval Oceanographic and Atmospheric Research Laboratory Ocean Science Directorate Stennis Space Center, MS 39529-5004	**10. Sponsoring/Monitoring Agency Report Number.** JA 331:042:91

11. Supplementary Notes.
Published in the Journal of Atmospheric and Oceanic Technology

12a. Distribution/Availability Statement. Approved for public release; distribution is unlimited.	**12b. Distribution Code.**

13. Abstract *(Maximum 200 words).*

A theoretical model of expendable bathythermograph (XBT) fall rate is reviewed, and a new form of fallrate equation is proposed to include near-surface transient effects. Comparisons are made of T-7 XBT and CTD (conductivity, temperature, and depth) depths of thermohaline features off Barbados. Fall-rate equation coefficients are derived and compared with the manufacturer-supplied coefficients. As other investigators have found, the Sippican equation consistently underestimates probe depth by as much as 35 m at 760 m. Analysis yields a new equation, $Z = 6.798t - 0.002383t^2 - 4.01$, for depths greater than about 10 m. Considerable probe-to-probe variability is noted and is found to be primarily the result of differences in the linear term or terminal velocity of the probes; variation in effective drag resulting from probe irregularities is the likely cause. Recommendations for additional work are made.

14. Subject Terms. Physical oceanography, expendable bathythermograph, expendable sensors	**15. Number of Pages.** 14
	16. Price Code.

17. Security Classification of Report. Unclassified	**18. Security Classification of This Page.** Unclassified	**19. Security Classification of Abstract.** Unclassified	**20. Limitation of Abstract.** SAR

The Fall Rate of the T-7 XBT

ZACHARIAH R. HALLOCK AND WILLIAM J. TEAGUE

92   8 24 033

The Fall Rate of the T-7 XBT

ZACHARIAH R. HALLOCK AND WILLIAM J. TEAGUE

DTIC QUALITY INSPECTED 5

The Fall Rate of the T-7 XBT*

ZACHARIAH R. HALLOCK AND WILLIAM J. TEAGUE

Naval Oceanographic and Atmospheric Research Laboratory, Stennis Space Center, Mississippi

ABSTRACT

A theoretical model of expendable bathythermograph (XBT) fall rate is reviewed, and a new form of fall-rate equation is proposed to include near-surface transient effects. Comparisons are made of T-7 XBT and CTD (conductivity, temperature, and depth) depths of thermohaline features off Barbados. Fall-rate equation coefficients are derived and compared with the manufacturer-supplied coefficients. As other investigators have found, the Sippican equation consistently underestimates probe depth by as much as 35 m at 760 m. Analysis yields a new equation, $Z = 6.798t - 0.002383t^2 - 4.01$, for depths greater than about 10 m. Considerable probe-to-probe variability is noted and is found to be primarily the result of differences in the linear term or terminal velocity of the probes; variation in effective drag resulting from probe irregularities is the likely cause. Recommendations for additional work are made.

1. Introduction

The expendable bathythermograph (XBT) was introduced by the Sippican Corporation in 1965. Since then it has become a widely used method of determining temperature profiles in the ocean, and is often depended on as a primary observational tool. There has been recurrent interest in improving the accuracy of XBT measurements, particularly the determination of probe depth. Since XBT depth is not measured directly but inferred from elapsed time and a fall-rate model, a number of factors affect the accuracy of the result. That these factors are variable has been documented by several investigators whose results have been summarized by Singer (1990) in his Table 3. In the present study we examine the fall-rate model and the variability of factors affecting it with a suite of comparison data.

The depths of most expendable probes [i.e., XBTs, expendable sound velocimeters (XSVs), expendable current profilers (XCPs)] are usually calculated using an equation of the form

$$Z = bt - at^2, \qquad (1)$$

where t is time elapsed from probe entry into the water. Since about 1974 it has been recognized that this equation has some inadequacies, particularly in the values of the coefficients. Singer (1990) provides a concise summary of past evaluations of Eq. (1) for the T-7

Corresponding author address: Dr. Zachariah R. Hallock, Department of the Navy, Naval Oceanographic and Atmospheric Research Laboratory, Stennis Space Center, MS 39529-5004.

XBT. In all cases it was found that the manufacturer-supplied coefficients ($a = 0.00216$ m s^{-2}, $b = 6.472$ m s^{-1}) are systematically too small.

In the present study we examine T-7 XBT and concurrent CTD (current, temperature, and depth) temperature profiles acquired in a region near Barbados, where the thermohaline structure of the upper water column is ideal for such comparisons. The purpose of the study is to further examine the validity of Eq. (1) for determining XBT depth. In section 2 we review the theoretical basis for Eq. (1) presented by Green (1984), hereafter G84, and suggest a modification to the fall-rate equation (FRE). Section 3 is a brief synopsis of previous studies of the XBT fall-rate problem. In section 4 we describe field measurements and present an analysis of the resulting XBT and CTD data and discuss implications for the FRE. Finally, in section 5, we make some recommendations for additional work that will be required if real improvements to expendable-probe depth accuracies are to be made.

2. XBT fall rates: A simple model

While processes involved in the descent of an expendable probe may be quite complex in detail, a relatively simple analytical model can describe most of the observational results. The model is that described by G84, and is presented here in a somewhat simplified way. A balance is assumed involving the vertical acceleration, the net buoyant force, and the hydrodynamic drag, the last being proportional to the square of the speed,

$$\frac{d^2Z}{dt^2} = \frac{g(m - m_w)}{m} - \frac{\rho_w C_D A W^2}{2m}, \qquad (2)$$

where Z is vertical position (positive downward) and

ρ_w = water density
C_D = drag coefficient
A = effective cross-sectional area of probe
W = vertical speed
m = mass of probe
m_w = mass of displaced water
g = acceleration of gravity
t = time.

The parameters in Eq. (2) can be expected to vary from region to region (ρ_w, m_w, C_D) and from probe to probe (m, C_D, A). Furthermore, it is clear that m varies with depth (as expendable probe wire unreels), and it is likely that C_D, m_w, and ρ_w will vary with depth, as well. Equation (1) implicitly assumes that the left side of Eq. (2) is negligible; here fall speed is assumed to be virtually equal to the terminal velocity, although the latter may change slowly with depth. This assumption is reasonable for depths in excess of about 10 m (G84), and we define this balance as asymptotic case 1. In this case,

$$W^2 = \frac{2g(m - m_w)}{\rho_w C_D A} = \frac{2gm'}{\rho_w C_D A}, \tag{3}$$

where $m' = m - m_w$. The parameters ρ_w, C_D, and m' can vary with depth. The last of these varies as a result of loss of XBT wire as the probe falls. The variation of W^2 due to the change in water density with depth is at most about 10% of that due to wire payout, and will be neglected here. The drag coefficient also can vary; the character and magnitude of this change is as yet a matter of controversy (G84).

Wire payout is effectively modeled as a linear function of depth:

$$m' = m_0'(1 - \epsilon Z). \tag{4}$$

Based on G84 and discussions with the manufacturer we estimate $\epsilon = 1.29 \times 10^{-4}$ m^{-1}. Following G84 we also model the variation in C_D as a linear function of depth:

$$C_D = C_{D0}(1 + \delta Z). \tag{5}$$

Then, taking the linear terms of an expansion,

$$W^2 \approx \frac{2gm_0'}{\rho_w C_{D0} A} (1 - \epsilon Z - \delta Z) \equiv W_T^2(1 - \eta Z), \tag{6}$$

where $\eta = \epsilon + \delta$. This can be directly integrated to yield depth of the probe as a function of time,

$$\int \frac{dZ}{(1 - \eta Z)^{1/2}} = W_T t + C, \tag{7}$$

where $W_T^2 \equiv 2gm_0'/\rho_w C_{D0} A$. Upon evaluation of the integral,

$$\frac{-2(1 - \eta Z)^{1/2}}{\eta} = W_T t + C. \tag{8}$$

If we take $Z(0) = 0$, then $C = -2/\eta$, and

$$Z = \frac{-\eta W_T^2 t^2}{4} + W_T t, \tag{9}$$

which is the result obtained by G84 and is the same form as Eq. (1). The quadratic term depends on the basic (initial) terminal velocity and on the parameter η (which depends primarily on the probe's mass loss due to wire payout). Using the manufacturer-supplied coefficients we can estimate η:

$$\frac{\eta W_T^2}{4} = 0.00216$$

$$W_T = 6.472,$$

so $\eta = 2.06 \times 10^{-4}$. Then from Eq. (6)

$$\delta = \eta - \epsilon = (2.06 - 1.29) \times 10^{-4} = 7.7 \times 10^{-5}.$$

For $Z = 10$ m ($t \approx 1.5$ s), the contribution of the quadratic term is only about 0.5 cm. Hence, for this shallow depth interval we examine asymptotic case 2, where we ignore variations in parameters, but do include the acceleration term. We rewrite Eq. (2) as

$$\frac{d^2 Z}{dt^2} = \frac{dW}{dt} = \beta - \alpha W^2, \tag{10}$$

where

$$\alpha = \frac{\rho_w C_D A}{2m}$$

$$\beta = \frac{gm'}{m}$$

and

$$W_T = \left(\frac{\beta}{\alpha}\right)^{1/2} = \left(\frac{2gm'}{\rho_w C_D A}\right)^{1/2}$$

(as before). Rearranging:

$$\frac{dW}{W_T^2 - W^2} = \alpha dt. \tag{11}$$

The integral of this is

$$\frac{1}{W_T} \left[\begin{array}{c} \coth^{-1}\left(\dfrac{W}{W_T}\right) \\[2mm] \tanh^{-1}\left(\dfrac{W}{W_T}\right) \end{array} \right] = \alpha t + C \quad \left(\begin{array}{c} \dfrac{W}{W_T} > 1 \\[2mm] \dfrac{W}{W_T} < 1 \end{array} \right). \tag{12}$$

Note the two regimes that depend on the ratio W/W_T (there is a singularity for $W = W_T$).

Applying the initial condition at $t = 0$ where W

$= W_0$ we evaluate C. After some rearranging we then have

$$W = W_T \begin{bmatrix} \coth(\alpha W_T t + C_1); & \dfrac{W_0}{W_T} > 1 \\[2ex] \tanh(\alpha W_T t + C_2); & \dfrac{W_0}{W_T} < 1 \end{bmatrix}, \quad (13)$$

where $C_1 = \coth^{-1}(W_0/W_T)$ and $C_2 = \tanh^{-1}(W_0/W_T)$. Equation (13) is then integrated to find $Z(t)$. After applying the condition $Z(0) = 0$, we obtain

$$Z = \frac{1}{\alpha} \left\{ \begin{array}{ll} \ln\left[\dfrac{\sinh(\alpha W_T t + C_1)}{\sinh C_1}\right]; & \dfrac{W_0}{W_T} > 1 \\[3ex] \ln\left[\dfrac{\cosh(\alpha W_T t + C_2)}{\cosh C_2}\right]; & \dfrac{W_0}{W_T} < 1 \end{array} \right\}. \quad (14)$$

Table 1 lists W, Z, and $\Delta Z = Z - W_T t$ for three cases of W_0. The largest absolute values of ΔZ are seen for $W_0 = 0$ and suggest an offset of about 4 m to be applied deeper than about 10 m when using Eq. (1) to calculate depth. If W_0 is close or equal to W_T this transient effect is minimal and ΔZ will be close to zero. The T-7 XBTs are typically dropped from about 2 m above the sea surface, which should (assuming a clean, vertical entry) result in an entry velocity close to the nominal value of W_T, about 6.5 m s^{-1}. Other factors not modeled, such as spinup of the probe, nonvertical entry, and air entrapped in the wire spool may also slow the probe in the first few meters.

It can be shown that for t sufficiently large (about 1.5 s for nominal parameters) such that Z is of the order of 10 m or larger, Eq. (14) approaches the form

$$Z = W_T t + D,$$

where D (the offset) depends on the initial speed, W_0. Here D is negative for $W_0 < W_T$ and positive for the reverse. For $W_0 = W_T$, $D = 0$. We have shown that for t of the order of 1.5 (or less) the quadratic term in

Eq. (1) is negligible. Hence, it is reasonable to propose a combined FRE as

$$Z = Z_1(t, W_0) - \frac{W_T^2 \eta t^2}{4}, \quad (15)$$

where Z_1 is just Eq. (14). A relationship between W_0 and D can be derived from Eq. (14), valid for all positive values of the ratio W_0/W_T:

$$\frac{W_0}{W_T} = 2 e^{\alpha D} - 1, \quad (16)$$

or

$$D = \frac{1}{\alpha} \ln \frac{(W_0/W_T) + 1}{2}.$$

Hence, an apparent W_0, based on an empirically determined value of D, can be used in Eq. (15) to determine Z. The minimum value for D (for a given α) is just

$$D_{\min} = \frac{\ln(0.5)}{\alpha} = \frac{-0.6931}{\alpha}, \quad (17)$$

which occurs for $W_0 = 0$.

3. Previous XBT fall-rate studies

Attempts to improve the XBT FRE are not new. McDowell (1977), Fedorov et al. (1978), and Flierl and Robinson (1977) discuss systematic offsets of isotherm depths derived from XBT and CTD data. The errors they found were generally of the same form and magnitude. This suggested a possible error in the manufacturer's FRE coefficients. Seaver and Kuleshov (1982) proposed a somewhat complex scheme to correct XBT depths. They considered the effects of temperature and salinity on drag. Heinmiller et al. (1983) also observed this systematic error and proposed a scheme to correct T-7 XBT depths. This was a piecewise linear correction to the recorded depth, with two segments meeting at 325 m; the error profile (i.e., Z_{XBT}

TABLE 1. Depth [From Eq. (14)], fall rate [from Eq. (13)], and $\Delta Z = Z - W_T t$ for three values of W_0, $\alpha = 0.1835$ m^{-1}, $\beta = 7.675$ m s^{-2}, and $W_T = 6.467$ m s^{-1} (parameter values adapted from G84).

Time (s)	$W_0/W_T = 0$			$W_0/W_T = 0.5$			$W_0/W_T = 2$		
	Z	W	ΔZ	Z	W	ΔZ	Z	W	ΔZ
0.00	0.00	0.000	0.00	0.00	3.234	0.00	0.00	12.936	0.00
0.40	0.59	2.859	−1.99	1.68	4.990	−0.91	4.04	8.384	1.46
0.80	2.16	4.783	−3.02	3.87	5.853	−1.30	7.11	7.148	1.93
1.20	4.29	5.759	−3.47	6.30	6.223	−1.46	9.87	6.723	2.10
1.60	6.69	6.184	−3.66	8.82	6.372	−1.53	12.52	6.566	2.17
2.00	9.21	6.357	−3.73	11.38	6.431	−1.55	15.13	6.506	2.19
2.40	11.76	6.425	−3.76	13.96	6.454	−1.56	17.73	6.483	2.20
2.80	14.34	6.451	−3.77	16.54	6.462	−1.57	20.32	6.474	2.21
3.20	16.92	6.462	−3.78	19.13	6.466	−1.57	22.91	6.470	2.21
3.60	19.51	6.466	−3.78	21.72	6.467	−1.57	25.49	6.469	2.21

$- Z_{CTD}$) appeared to be roughly linear in the two regimes. They suggested that some of the error may have been due to the analog recordings used at the time. Hanawa and Yoritaka (1987) discussed FRE coefficient modification based on data from Japanese-made XBTs and a digital acquisition system. They used a regression analysis that resulted in coefficients larger than those of the manufacturer. The error profile they found was nearly linear, unlike those found previously.

Wright and Szabados (1989) examined the FRE for the T-7 (among others) with data acquired in the same region as the present study. They also found that the manufacturer's FRE underestimates depths of thermal features observed with concurrent CTD casts. They used a regression scheme that adjusted the apparent sampling time interval of the XBTs to minimize the error profile. The procedure led to correction factors for the FRE coefficients. Their results differed from those of Hanawa and Yoritaka (1987) by about 11 m at a depth of 750 m. Since these datasets were acquired in different oceans with probes manufactured in different countries, some differences should be expected.

Singer (1990) presented a summary of previous studies of the T-7 FRE and compared them to results using data from the Gulf of Mexico. His FRE coefficients fall between those found by Hanawa and Yoritaka (1987) and Wright and Szabados (1989). Singer also found an offset term (about 4 m) for his quadratic FRE; he stated that this offset was ". . . an artifact of the linear fit . . ." which, unlike other investigators' equations, had not been found to fit to zero depth at zero time. Indeed, we infer that the fall rate is not linear close to the surface, as is also suggested by Eq. (15).

4. Observations

In this section we briefly describe (a) a test-and-evaluation experiment involving CTD and XBT measurements. We then describe (b) comparisons and analyses of these data and the determination of new FRE coefficients using selected features in the temperature profile, and we subsequently discuss (c) the variability of individually determined (for each XBT probe) FRE coefficients. Finally (d) we examine the implications of the new FRE for the entire XBT range.

a. Data

In May 1990 we conducted CTD–expendable-probe comparisons near 16°N, 56°W, about 300 nm northeast of Barbados. The thermohaline structure of the upper 100 m in this region consists of large, well-defined, and persistent "staircases" (alternating isothermal, isohaline layers and high-gradient "sheets"). These characteristics are ideal for comparisons of hydrographic profiling systems. These structures are particularly useful in the present case because depth uncertainties can be effectively decoupled from; for ex-

ample, temperature uncertainties. In this paper we describe a subset of the data acquired during the overall experiment.

Over a period of about 2 h, 36 sets of 4 simultaneous T-7 XBTs were dropped using four Sippican Mark-9 Launcher Acquisition Systems (LAS's). Concurrently, five CTD casts were made to about 1000 m with a Neil Brown, Mark III CTD system. During this period, the ship was dead in the water and conditions were good.

The CTD was calibrated at the Naval Oceanographic Office before the cruise. Temperature error was found to be less than 0.003°C, and pressure uncertainty was less than 4 db between 0 and 1000 db. Additionally, a short time series (about 10 min) of CTD data collected with the probe at a measured average depth of 4 m resulted in an average pressure of 2.5 db, indicating that the CTD pressure was too low by 1.5 db. CTD pressures were corrected by this amount prior to further analysis, and converted to depth by integrating the CTD-measured specific volume of seawater using a constant value of the acceleration of gravity of 9.8 m s^{-2}. Of the 144 probes (T-7's) dropped between about 0545 and 0800 UTC only 128 were recorded. Data from 16 probes were lost as a result of acquisition system malfunction; most of these (14) losses occurred on LAS 3. Of the recorded data, 10 probes (8%) produced bad temperature data or ended early (broken wire). A typical set of simultaneous XBT temperature profiles is shown in Fig. 1. Superimposed (dashed curve) is a concurrent (time-interpolated) CTD temperature profile. Since CTD and XBT temperatures were sampled at different times at each depth due to the sampling scheme and widely different descent rates and since the thermal field was changing on short periods due probably to internal wave straining, time interpolation of the CTD data was necessary. In particular, depth-interpolated CTD profiles were interpolated in time to coincide with XBT sample times (the time-interpolation procedure is further explained next).

Two things are immediately evident in Fig. 1. The CTD data show the step features significantly deeper than do the XBT data, consistent with comparisons made previously (Hanawa and Yoritaka 1987; Wright and Szabados 1989; and Singer 1990). The simultaneously dropped XBTs show differences in feature depths among themselves. The latter observation holds to a greater or lesser extent (than the case shown in Fig. 1) for all simultaneous sets of XBTs.

b. Regressions based on selected feature depths

To better quantify the depth discrepancies, expanded plots of segments of the profiles containing identifiable features were examined. For the example (Figs. 2a,b) depth discrepancies between simultaneous XBT profiles exhibit both overall offsets and depth dependencies. Also evident are temperature offsets in the isothermal layers (up to about 0.1°C in the example).
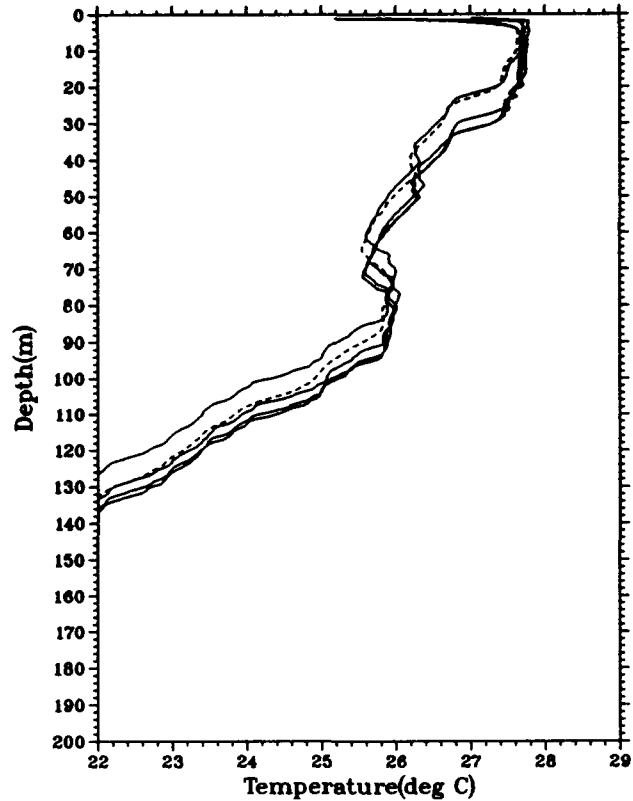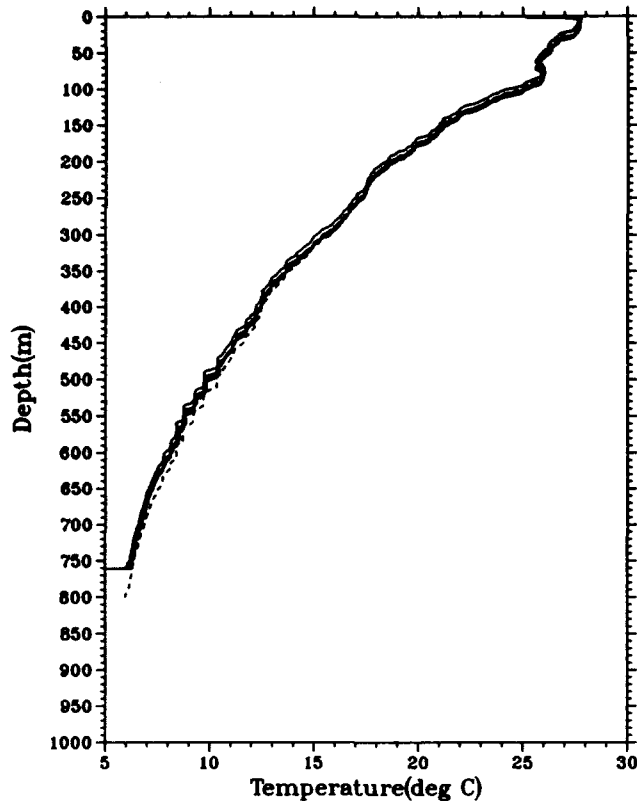
FIG. 1. Typical set of simultaneous XBT profiles (solid curves) and time-interpolated CTD profile (dashed) of temperature.

Most such temperature offsets in these data were within the manufacturer's tolerance of 0.2°C, but they made automated analysis algorithms difficult to formulate (some of the temperature errors were functions of depth). Hence, we decided to identify manually a set of features that were common to all XBTs and CTDs. Figures 3a,b show the 16 features selected on one of the example XBTs. The depths of these points were manually digitized with a resulting estimate of ±1 m digitization error. Rather than digitizing the time-interpolated CTD profiles (such as that shown in Figs. 1 and 2) the five original CTD temperature profiles were digitized and the feature depths subsequently interpolated to respective XBT times. The time-interpolation scheme assumed an average CTD descent rate of 1.02 ± 0.04 m s^{-1} (based on actual CTD profiles) yielding an uncertainty in the time of interpolated Z_{CTD} of about 1 min (the same scheme was used to time interpolate the full CTD profiles discussed previously). XBT data were recorded as depth and temperature so the time of each XBT sample was calculated by inverting the manufacturer's FRE:

$$t_{XBT} = 1498[1 - 0.5(1 - 2.0627 \times 10^{-4} Z_{XBT})^{1/2}],$$
(18)

where Z is the depth in meters and t is in seconds. Time interpolation provided a CTD depth for each
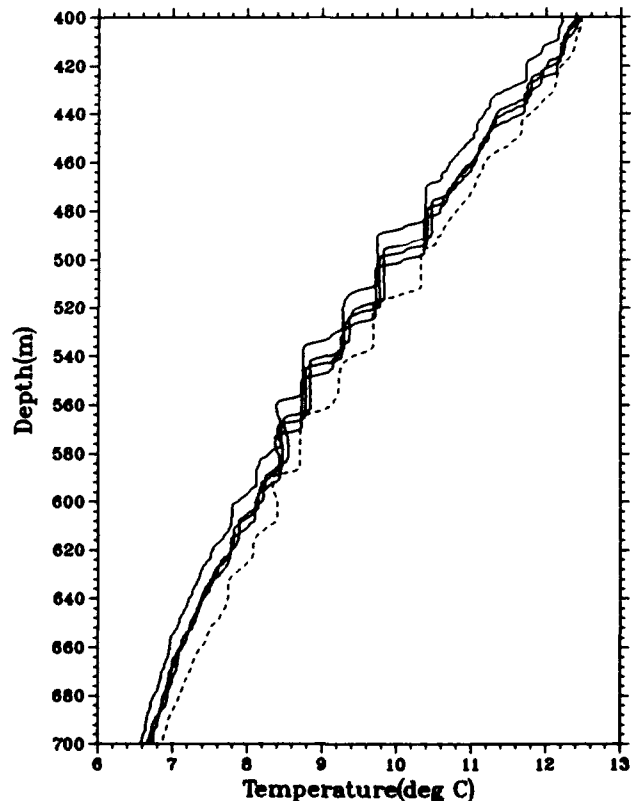

FIG. 2. Typical set of simultaneous XBT profiles (solid curves) and time-interpolated CTD profile (dashed) of temperature: (a) upper 140 m, (b) 400–700 m.
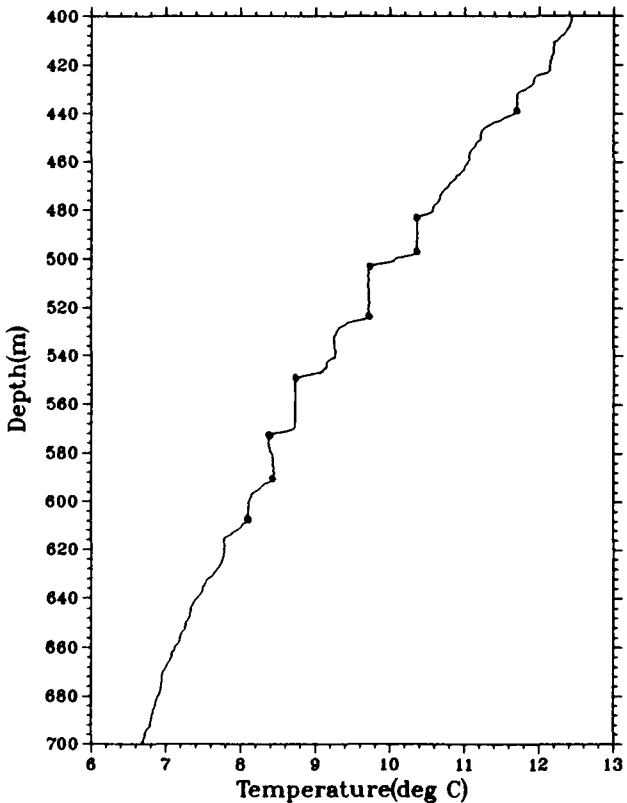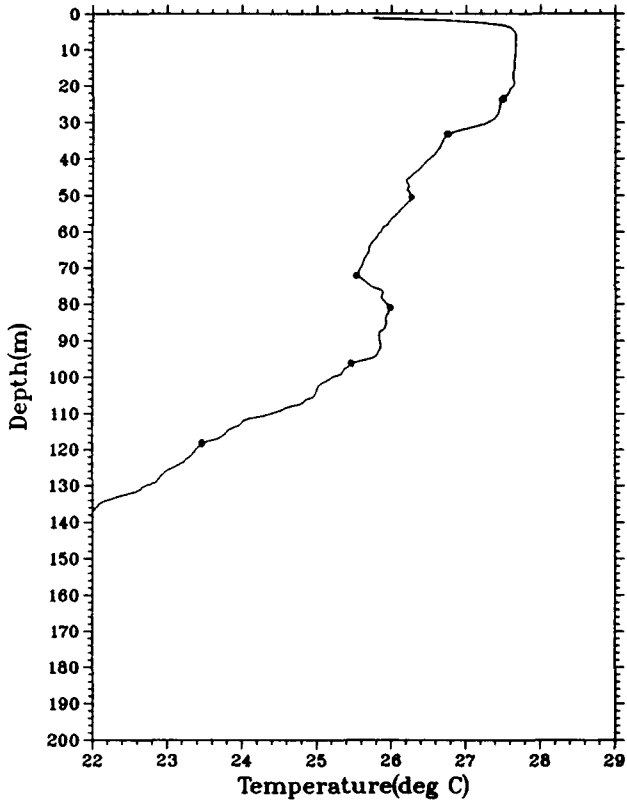
FIG. 3. Typical XBT profile showing selected features (dots) used in the analysis: (a) upper 140 m, (b) 400–700 m.

XBT group, i, and each feature, j. Similarly, for each feature and XBT group we have a set of up to four XBTs, k. Hence, $Z_{CTD}(i, j)$ is a function of $t_{XBT}(i, j, k)$ for $i = 1, 36; j = 1, 16; k = 1, k_{max} \leq 4$, where we take Z_{CTD} to be the "correct" feature depth, and XBT depths with their errors are expressed as t_{XBT} through Eq. (18).

Depth errors $(Z_{CTD} - Z_{XBT})$ for all features are plotted as functions of Z_{CTD} in Fig. 4. An offset of approximately 4 m near the surface and the positive bias at depth reported by other investigators are apparent. Additionally, the large scatter suggested by the profile plots is greater at depth than near the surface. Of these differences, 67% exceed the manufacturer's cited tolerance of 2% of depth or 5 m.

The manufacturer's FRE [Eq. (1)] is quadratic in time but contains no constant term; it is of the same form as Eq. (9) for asymptotic case 1. To account for possible offsets resulting from transient effects as in asymptotic case 2 or some other systematic data offset, we included an unspecified constant term and sought all three coefficients by least-squares analysis. That is, we minimized

$$E^2 \equiv \overline{(Z - \hat{Z})^2}, \tag{19}$$
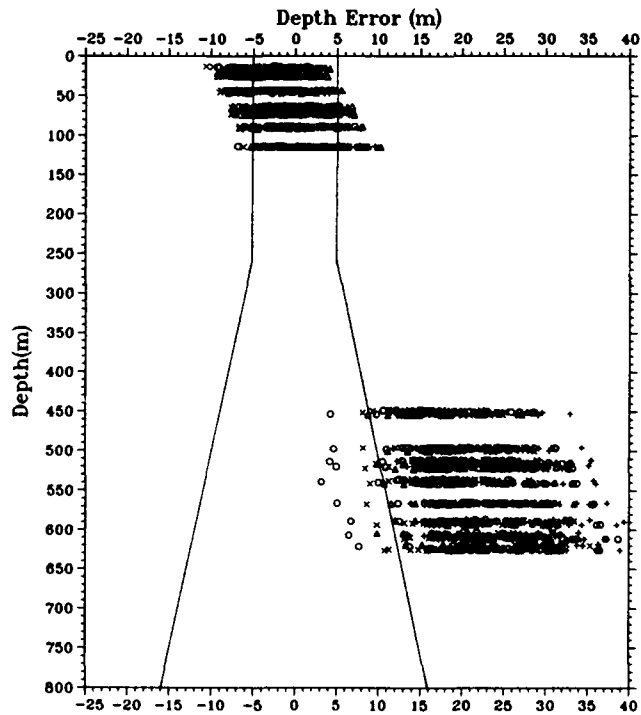
where

$$Z = Z_{CTD}(i, j) \tag{20}$$

FIG. 4. Depth error $(Z_{CTD} - Z_{XBT})$ for selected features. XBT depths calculated with the Sippican FRE. Different symbols denote different LAS's.

TABLE 2. Fall-rate equation coefficients from regression analysis with uncertainty error e and overall rms error of fit E.

	a (m s^{-2})	e (%)	b (m s^{-1})	e (%)	c (m)	e (%)	E (m)
Case 1 (fully quadratic)	0.00409	5.7	6.962	0.32	−5.53	4.1	5.18
Case 2 (modified)	0.00238	—	6.798	0.05	−4.02	3.7	5.25

and

$$\hat{Z} = -at^2_{\text{XBT}}(i, j, k) + bt_{\text{XBT}}(i, j, k) + c. \quad (21)$$

The overbar denotes an average over a set of Z, t pairs.

In the first case we averaged over all 118 good profiles and all 16 features in each profile (a 1888-member average). Coefficients resulting from a straightforward regression, with associated errors, appear in Table 2. From Eq. (9) in section 1 we derived from these a value for η, the linear component of depth dependence of fall-rate parameters:

$$\eta = \frac{4a}{b^2} = \frac{4.102 \times 10^{-3} \times 4}{(6.95)^2} = 3.397 \times 10^{-4} \text{ m}^{-1}. \quad (22)$$

This is about 1.6 times the value implied by the original FRE. Since $\eta = \epsilon + \delta$ and $\epsilon = 1.29 \times 10^{-4}$ m^{-1} [Eq. (4)], $\delta = 2.1 \times 10^{-4}$ m^{-1}, an unreasonably large change of the drag coefficient (G84) is implied. Furthermore, the quadratic and linear coefficients are larger than those found by Wright and Szabados (1989) for the same region.

An alternative approach constrains the relationship between a and b by specifying a plausible value of η. Since we do not really know δ exactly, we use the value of η inferred from the original FRE, 2.06×10^{-4} m^{-1}. Here, a modified regression was performed using a specified, initial value for a. The coefficients b and c were found, and a new value of a was calculated using the fixed η and Eq. (22). This process was repeated until the coefficients converged to constant values (typically abut four iterations). These also appear in Table 2 (no uncertainty is presented for a here, since it is specified and dependent on b). The rms error in this case is only slightly greater than the error from the previous approach. Furthermore, the quadratic and linear coefficients are virtually identical to those found by Wright and Szabados (1989). Indeed, in their analysis, while apparently different from that presented here, the quadratic and linear terms were linked; they used only one free parameter, a sampling interval correction (they did not allow a constant offset). Hence, they effectively constrained their analysis to the original value of η, as has been done here.

The differences between depths calculated with the Sippican FRE and those calculated with the two FREs represented in Table 2, as well as FREs proposed by other investigators, are plotted as functions of depth in Fig. 5. The curve of our second FRE (Table 2) is

parallel to that of Wright and Szabados (1989), differing only by the offset term. Singer's (1990) equations [(3a) and (3b) of his Table 3] appear to yield quite similar results; his equations differ by 2 m at most (at 760 m), which is insignificant in the light of the uncertainties we found. Singer's Eq. (3a), the equations proposed by Hanawa and Yoritaka (1987) and Wright and Szabados, and our second equation exhibit nearly linear difference curves, differing only slightly in slope and offset. Our first equation is clearly the anomaly because of the relatively large quadratic coefficient. Our two equations agree at 65 and 561 m. There is a relative maximum discrepancy of about 2.5 m near a depth of 320 m and a maximum discrepancy at the bottom of the profile (760 m) of about 6 m (the disagreement between the derived equations and the Sippican equation exceeds 25 m at 760 m). With the rms error of fit for both derived equations greater than 5 m, there is no clear statistical basis for selecting one or the other of these sets of coefficients as the more correct. Since the second case constrains the quadratic and linear coefficients to be consistent with a reasonable physical model, we selected this case for all subsequent discussion. Future investigations should include efforts to refine estimates of the parameter η.

Singer (1990) summarized XBT fall-rate studies by other investigators. He found a similar negative offset (about 4 m) to that found here (the others apparently did not) and suggested that the probes may have fallen more slowly between the surface and 100 m than they did deeper than this level. An apparent lower descent rate near the surface, hence a negative offset term in the regression, would result if the probe were to begin its descent at less than its terminal velocity. We attempted to reconcile the observed offset term with the model described in section 2. A plausible value for α [in Eq. (17)] is 0.185 m^{-1} yielding $D_{\text{min}} = -3.7$ m. Hence, if the model implicit in Eq. (15) is relevant, W_0 would have to be zero. Since the probes were dropped from a height of 1.5–2 m above the surface, W_0 was probably close to W_T, suggesting that the model may be inadequate or that there may have been initial decelerations when the probes impacted the water.

Using the coefficients resulting from the modified regression analysis, XBT depths were recalculated. These depth errors for the features are plotted in Fig. 6. Now, 87% of the points fall within the cited tolerance (indicated by the lines on the plot). A similar calculation using the coefficients from the fully quadratic case produced a very similar distribution (not shown).
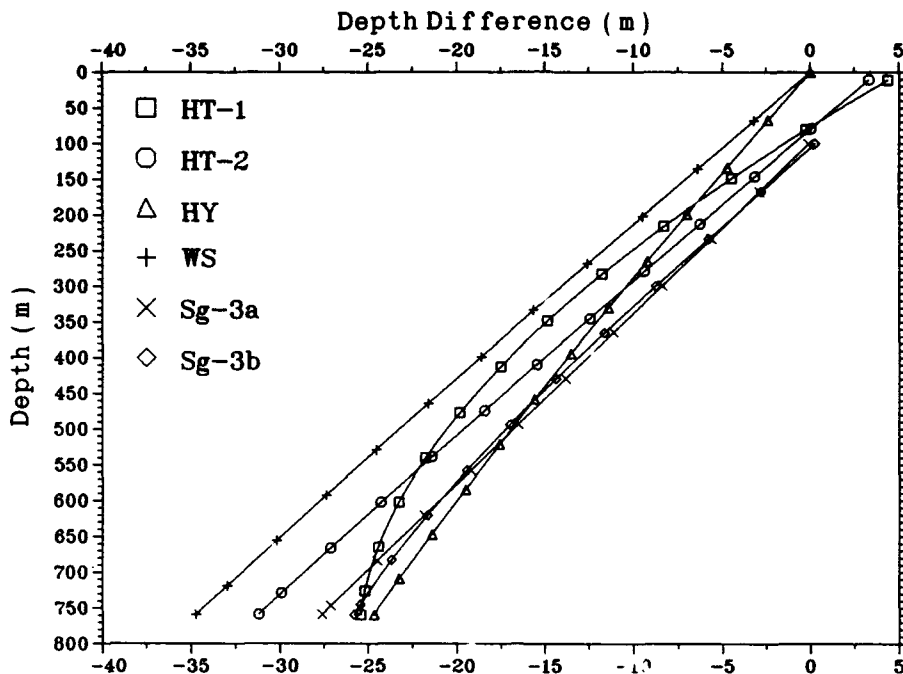
FIG. 5. Differences between depth calculated with the Sippican FRE and other FREs discussed in the text. Specifically $Z_{Sippican} - Z_i$, where i = HT-1 (first equation of Table 2), HT-2 (second equation of Table 2), HY (Hanawa and Yoritaka 1989), WS (Wright and Szabados 1987), Sg-a [Singer 1990, Eq. (3a)], Sg-b [Singer, Eq. (3b)].
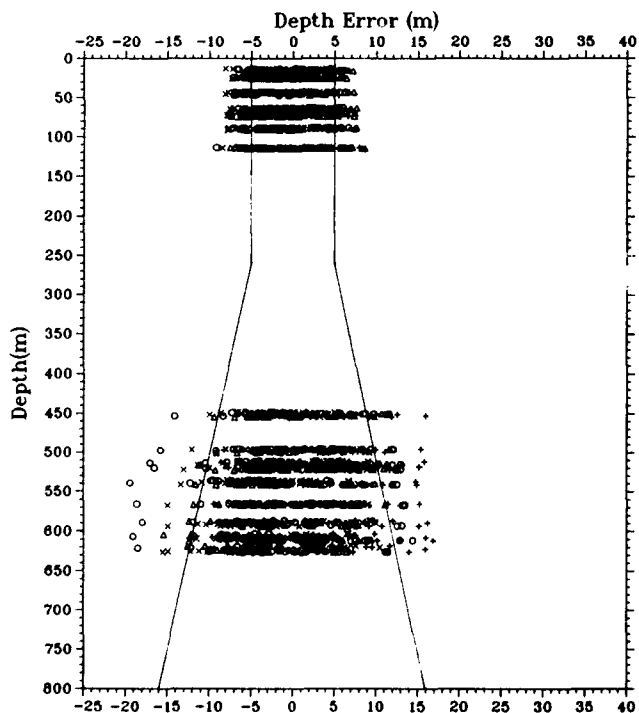

FIG. 6. Depth error ($Z_{CTD} - Z_{XBT}$) for selected features, XBT depths calculated with coefficients resulting from modified overall regression ($Z_{XBT} = 6.798t - 2.38 \times 10^{-3}t^2 - 4.02$). Different symbols denote different LAS's.

What is quite apparent is that a great deal of variability remains from probe to probe, although the systematic skewing of depth errors (Fig. 4) has been removed.

c. Individual profile regressions and corrections

Toward a better understanding of the variability of depth errors, we conducted a modified regression analysis (with $\eta = 2.06 \times 10^{-4}$ m^{-1}), producing a set of coefficients for each profile. Subsequently, the depths in each profile were corrected using its respective set of coefficients, and depth differences were again plotted (Fig. 7); a significant reduction in the errors is apparent, but a slight trend remains in the deeper layers.

Analogous to Figs. 2a,b, the same set of simultaneous XBTs, with depths corrected with individually determined coefficients, is plotted in Figs. 8a,b. This is typical of all individually corrected XBTs and illustrates the empirical validity of the form of the FRE used. We conclude here that most of the variability from probe to probe is accounted for by variations in the linear and constant terms, and not in η; that one equation of the form (21) is adequate to represent the fall rate of the XBT for depths > 10 m; and that more complex equations involving higher-order terms are probably unnecessary.

It is useful to examine more closely the variability of the coefficients. Questions arise as to whether most
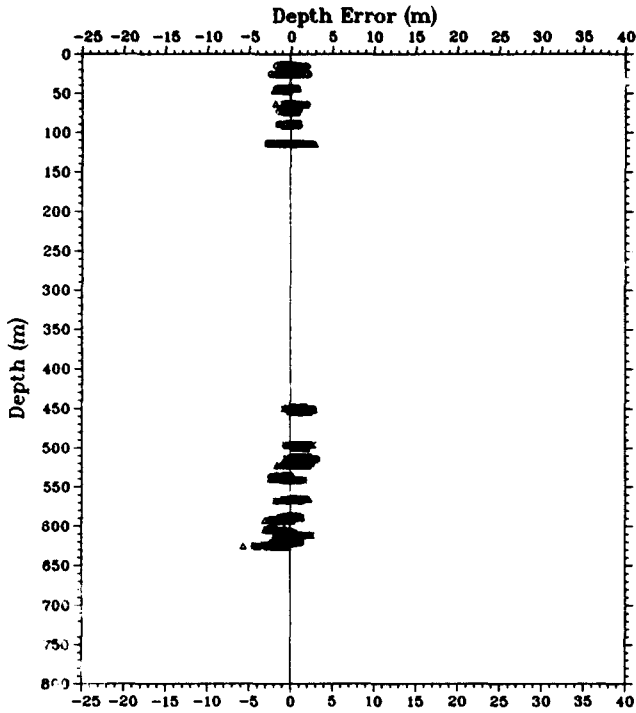
FIG. 7. Depth error ($Z_{CTD} - Z_{XBT}$) for selected features and XBT depths calculated using individually determined coefficients. Different symbols denote different LAS's.

of the variability is temporal, the result of differences in LAS problems, or just due to differences in the probes themselves. The coefficients (b and c) found using $\eta = 2.06 \times 10^{-3}$ m^{-1} are plotted as functions of time in Figs. 9 and 10. The different symbols in the figures denote which LAS is represented. There is no clear pattern to the variations in b and c. They are not correlated, and there appears to be as much variation between values for fixed times as there is for a given LAS as a function of time. For this dataset, much of the scatter in c can be attributed to a LAS malfunction (Sippican, personal communication) where the first few scans of data (the exact number is unknown and appears to be random) were lost at the beginning of each probe launch. Means and standard deviations of b and c quantities appear in Figs. 11 and 12. The right ordinate axis of Fig. 11 is in units of depth and represents the contribution of the linear term to the FRE at $t = 122$ s, the time in which the probe reaches about 760 m using the original Sippican coefficients. Also appearing is the rms spread, based on the maximum difference of b (and of c) within each simultaneous XBT group. There is no LAS dependence apparent for c, so the acquisition malfunction appears to have been ubiquitous. It should be noted here that XCTD probes launched from these same systems on the same cruise exhibited standard deviations in c of only about 1.5 m (Hallock and Teague 1990). For the XCTDs, the LAS's
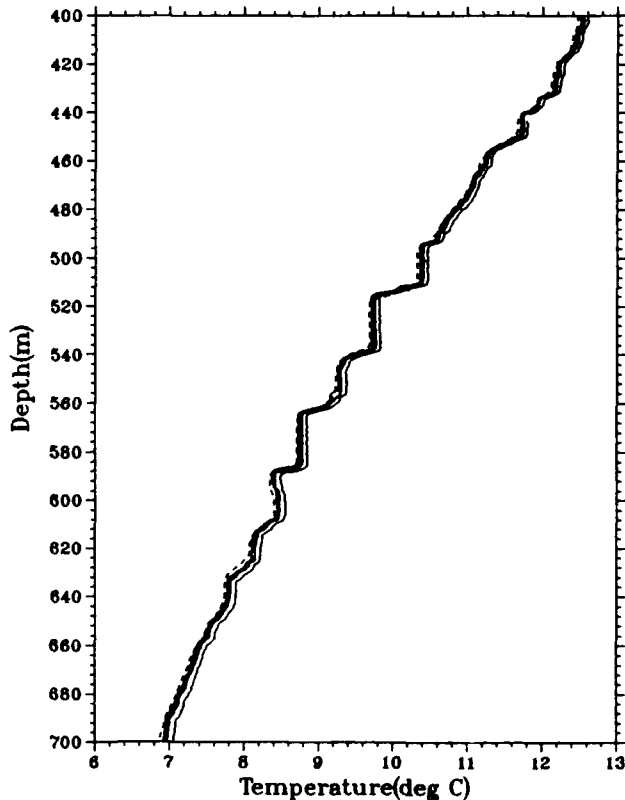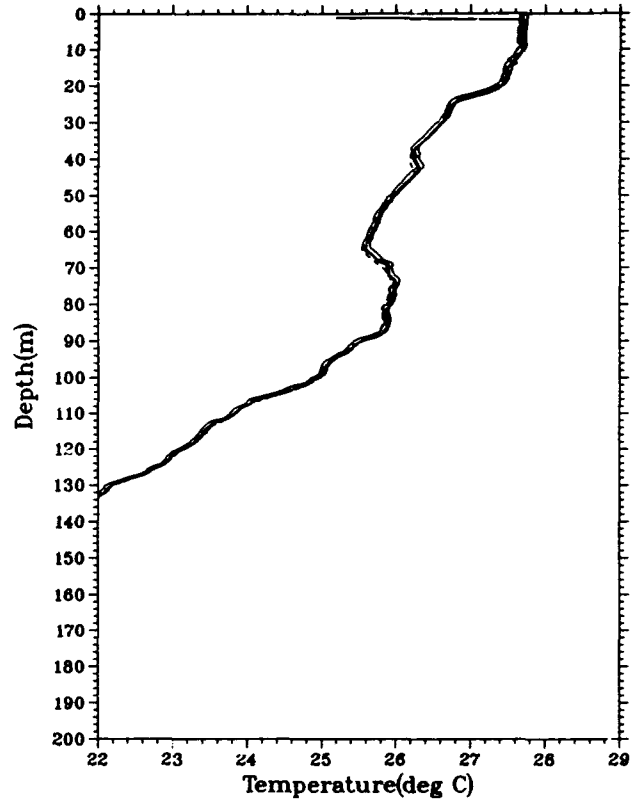

FIG. 8. Typical set of simultaneous XBT profiles (solid curves) with depths calculated with individually determined coefficients. Time-interpolated CTD temperature (dashed) is also plotted: (a) upper 140 m, (b) 400–700 m.
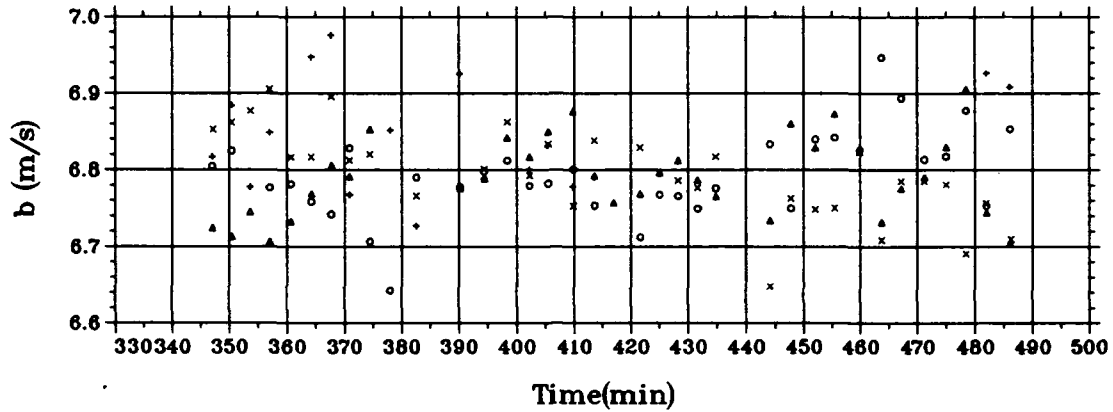
FIG. 9. Individually determined coefficient b. Different symbols denote different LAS's.

were in a different mode and data were not lost (Sippican, personal communication). Standard deviations and rms spread are virtually the same for b (and for c). The mean value of b for LAS 3 is barely significantly higher than for the other LAS's. Since there were only 18 XBT profiles acquired with LAS 3 (versus about 33 for the others), we suspected a bias due to the missing data. We recalculated the means of data acquired with LAS 1, LAS 2, and LAS 4 including only profiles corresponding to those from LAS 3; there were virtually no differences from the values appearing in Fig. 11. The reason for the anomalous mean b for LAS 3 is not clear.

For comparison, b from several other studies, as well as the Sippican value, also appears in Fig. 11. The value found by Singer (1990) is within the standard deviation envelopes for three of the four records of the present study. That of Hanawa and Yoritaka (1987) is barely outside the envelopes. This suggests that hypothesized regional differences in fall rates may not be statistically significant.

A portion of the variability in c (and perhaps part of the mean c as well) is the result of a data-acquisition problem. The remainder may well be due to acceleration of the probes within the first 10 m; differences in probe entry angle or other mechanical perturbations may contribute to the observed scatter. Unfortunately, we cannot separate the LAS problem from other effects with this dataset, so a definitive determination of a real offset for use in Eq. (15) awaits a future investigation. The primary cause of probe-to-probe variability is the coefficient b (or W_T). While overall or average values of b may vary due to environmental conditions (e.g., the density profile), probe-to-probe variability seen in the present study is most likely the result of differing probe weight, volume and/or effective drag. G84 concluded (based on actual measurements) that probe weight and volume probably cannot explain the variability, implying that differences in drag are the cause. These might include slight differences in roughness of the surfaces of the probes, affecting the separation point for turbulent layers.
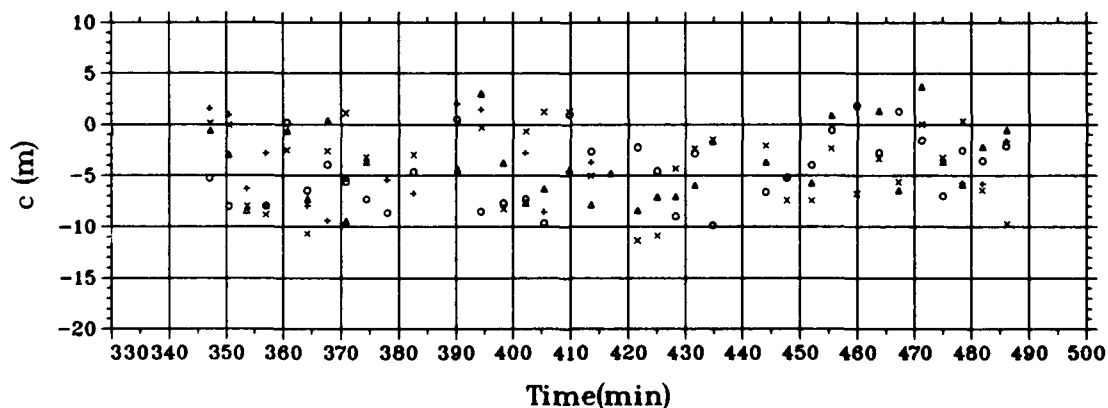

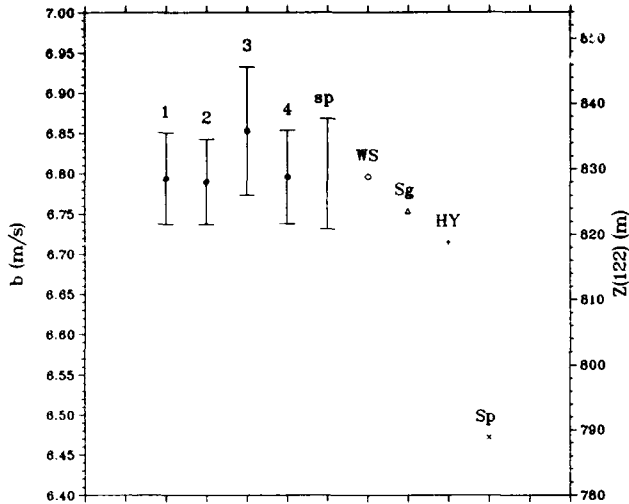FIG. 10. Individually determined coefficient c. Different symbols denote different LAS's.

FIG. 11. Means (dots) and standard deviations (error bars) of individually determined regression coefficients b for the four LAS's (labeled 1, 2, 3, 4); rms of maximum spread of b in simultaneous XBT groups (labeled sp). Also shown are values of b found by other investigators: WS—Wright and Szabados (1987), Sg—Singer (1990), HY—Hanawa and Yoritaka (1989), Sp—original Sippican value.

d. Implications for the entire temperature profile

The preceding analyses and dicussion were based on selected points of the temperature profile. These were chosen to avoid contamination of results by errors in measured temperature. The depth interval between about 150 m and 400 m and that deeper than about 630 m were not directly addressed. Hence, it was useful to assess the effectiveness of the new FRE (second set of coefficients in Table 2) in accurately representing
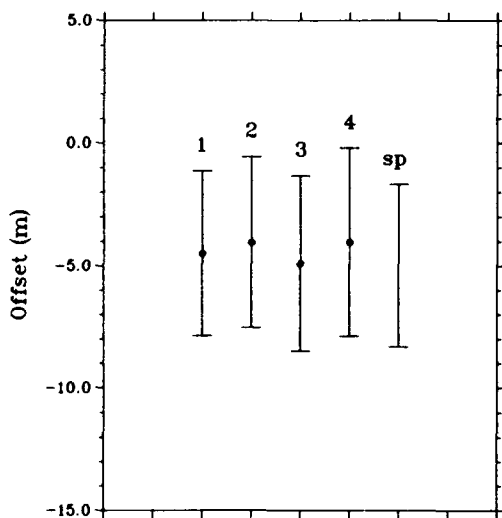

FIG. 12. Means (dots) and standard deviations (error bars) of individually determined regression coefficients c for the four LASs (labeled 1, 2, 3, 4); rms of maximum spread of c in simultaneous XBT groups (labeled sp).

the temperature profile over its entire depth range (10–760 m). To do this we formed an error profile

$$\delta T(Z) = T_{\text{CTD}}(Z) - T_{\text{XBT}}(Z) \qquad (23)$$

for each XBT profile. Here T_{CTD} is CTD temperature data interpolated to the time of the corresponding XBT sample (explained earlier). We then calculated mean and rms profiles by averaging over all 118 XBTs. For reference purposes we first examine the statistics of δT calculated using the uncorrected XBT profiles. Figure 13 (analogous to Fig. 4 for the depths of features) shows a mean-error profile that starts near $-0.2°$ near the surface, increases to a maximum near $0.4°$, and decreases again to about $0.12°C$. Superimposed on this overall trend are excursions of the order of $0.2°C$ over vertical scales of about 20 m. The rms error profile reflects primarily the mean. By recalculating XBT depths using the new FRE, we have removed most of the large-scale trend in δT (Fig. 13; analogous to Fig. 6) and have reduced the rms error to a considerable degree. The remaining error profile has two aspects of note: the same (but somewhat reduced) vertical structure near the surface and in the depth aperture containing the step features, and a nearly depth-independent negative offset of the mean error. We suggest that
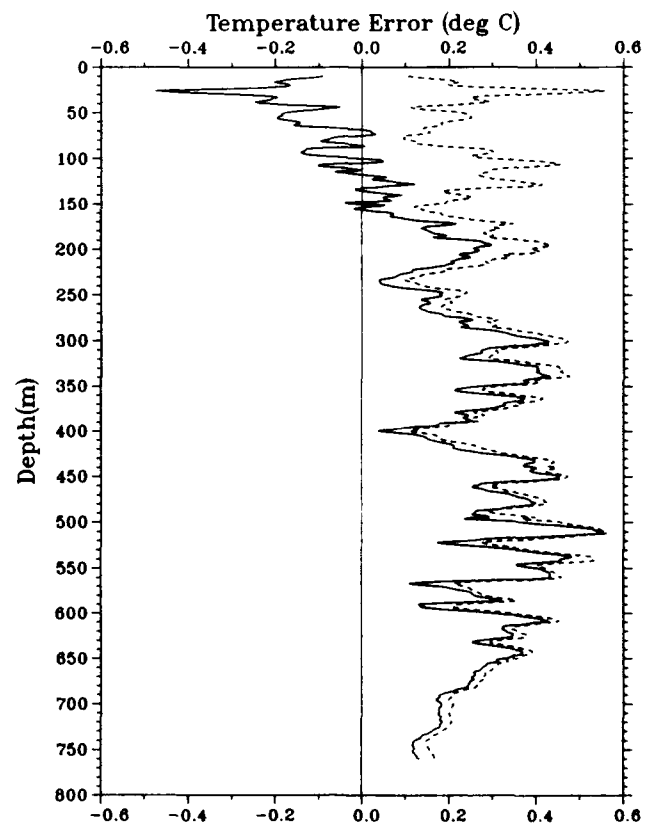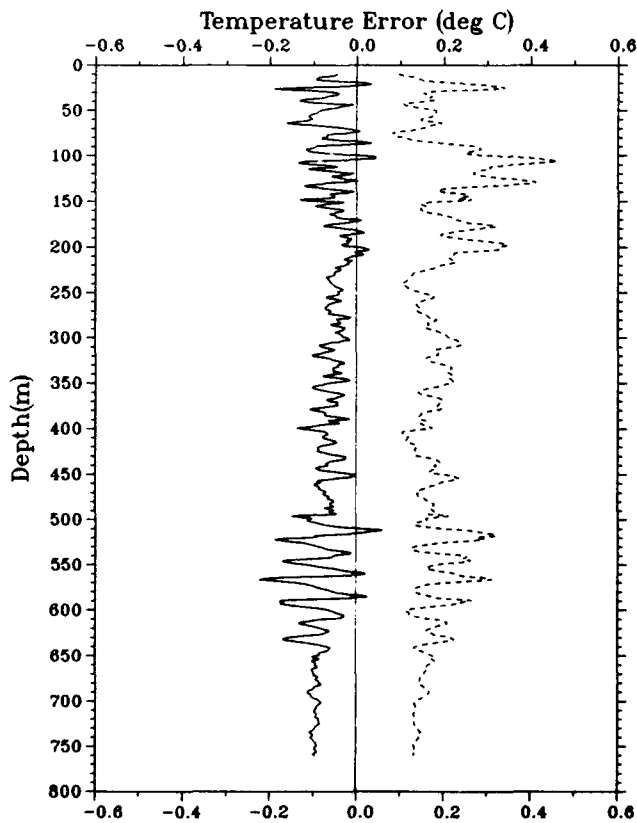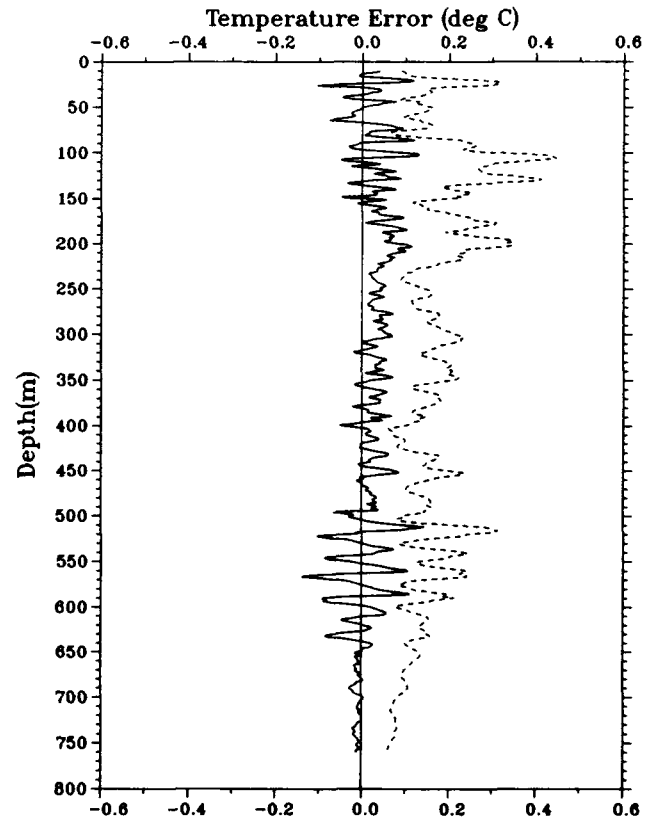

FIG. 13. Temperature error ($T_{\text{CTD}} - T_{\text{XBT}}$) mean (solid) and standard deviation (dashed) profiles for XBT depths calculated with the Sippican FRE.

the approximate 20-m vertical structure in the error profile is the result of probe-to-probe variability in fall-rate parameters as discussed in the preceding subsection. This hypothesis is addressed in the following. The nearly constant offset error cannot be the result of a residual error in the FRE coefficients since the temperature profile is not a linear function of depth. Examination of individual XBT error profiles (not shown) showed them to be primarily depth-independent offsets. The mean offset (Fig. 14) is about −0.1°C. This translates to an isotherm depth error, according to

$$\delta Z = (\partial T/\partial Z)^{-1}\delta T. \tag{24}$$

Near the bottom of the profile, $\partial T/\partial Z \approx 10^{-2}\,°C\,m^{-1}$, yielding $\delta Z \approx 10$ m. Individual offsets can be nearly twice this value.

` To eliminate any ambiguity as to the source of the temperature offset error, we used an approach analogous to that used to calculate the FRE coefficients. Here, however, we identified eight points in the CTD temperature profiles that were relatively isothermal in depth and time. The characteristics of these features are summarized in Table 3. Six of the points were in the virtually isothermal layers below the steps used in

TABLE 3. Selected temperature calibration points.

Z_{CTD} (m)	T_{CTD} (°C)	$\sigma_{T_{CTD}}$ (°C)
8	27.64	0.02
83	25.83	0.01
446	11.66	0.00
507	10.32	0.01
530	9.69	0.00
551	9.22	0.01
572	8.71	0.01
595	8.35	0.02

the previous (FRE) analyses. The remaining two points were in the upper 100 m. The standard deviations for all selected points are less than 0.03°C. The same features were identified in the XBT profiles, and profiles of ΔT [defined as in Eq. (23) but for the selected points] were derived. The vertical gradients of XBT temperature for the selected points were at most $0.03°C\,m^{-1}$. We reemphasize here that ΔT found in this way is virtually independent of FRE errors. We then calculated an average (over depth) ΔT for each XBT and corrected each actual XBT profile with this average. Figure 15 depicts the error profile statistics following temper-

FIG. 14. Temperature error ($T_{CTD} - T_{XBT}$) mean (solid) and standard deviation (dashed) profiles for XBT depths calculated with the second FRE of Table 2 [Eq. (25)].

FIG. 15. Temperature error ($T_{CTD} - T_{XBT}$) mean (solid) and standard deviation (dashed) profiles for XBT depths calculated with the second FRE of Table 2 [Eq. (25)] and with corrected XBT temperatures.

ature correction (using the XBTs with depths calculated with the new FRE). Most of the offset error has been removed, and the rms error has been reduced somewhat below about 550 m.

Finally, to test the assertion made earlier than most of the remaining structure and variability in the error profile are the result of probe-to-probe variations in fall-rate parameters we further depth corrected each XBT with its respective individually determined FRE coefficients (as in the previous subsection). The resulting error profiles appear in Fig. 16 (analogous to Fig. 7). Indeed, most of the structure and variability are gone. The largest remaining errors occur between 100 and 250 m and are generally less than 0.1°C.

In summary, the proposed new FRE coefficients effect a significant improvement in temperature measurement capability over the full depth range of the T-7 XBT. Most of the remaining errors are due to individual physical probe differences and depth-independent temperature bias. A bulk, quantitative measure of the improvement is given in Table 4, which shows δT statistics computed over all XBTs and depth. The largest improvement is the decrease in the mean error, while the rms error was reduced by about 40%.
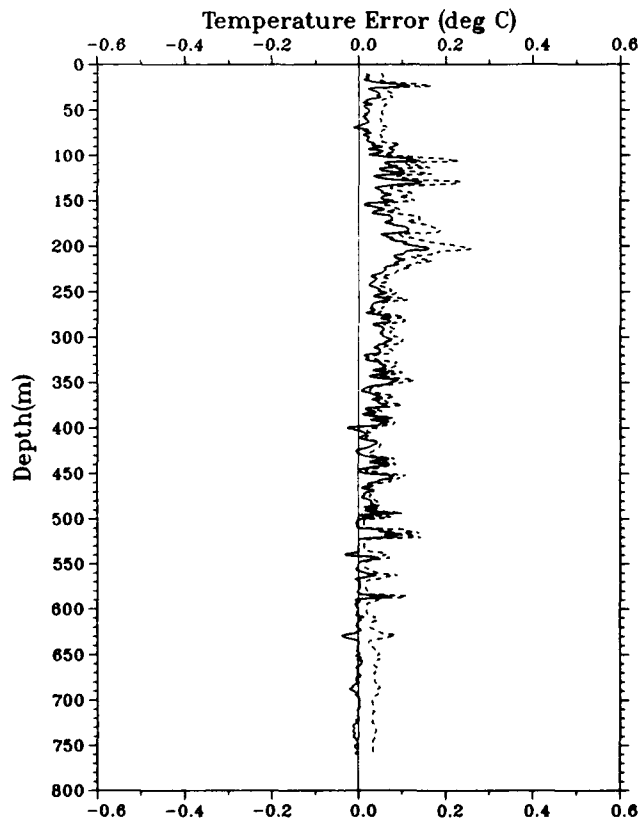
Table 4. Overall temperature errors.

FRE	$\overline{\delta T}$ (°C)	rms (δT) (°C)
Sippican	0.19	0.32
Proposed	0.07	0.19

5. Conclusions and recommendations

With the analysis of concurrent CTD and XBT temperature profile data acquired in the Atlantic Ocean near Barbados we have shown (as have others) that the presently used T-7 fall-rate equation is inadequate. An improved equation is proposed for depths greater than 10 m:

$$Z = 6.798t - 0.00238t^2 - 4.01. \quad (25)$$

This new equation reduces overall rms XBT-measured temperature error by about 30%. The rms residual depth error in the determination of the coefficients of Eq. (25) is about 5.2 m. Most of this error is the result of probe-to-probe differences in terminal velocities, which, in turn, are probably due to variations in probe-drag characteristics. The probe-to-probe variability diminishes the relative importance of differences in fall rates found in different studies, and is a caveat to investigators who use XBTs to examine finescale features. The remedy for the variability will first require determination of its cause. If it is the result of differences in effective drag, some way must be found to make the probes more uniform in this respect, perhaps involving mechanical design modifications.

We further propose a more complete equation that includes an initial acceleration in the upper 10 m,

$$Z = Z_1(t, W_0) - 0.00238t^2, \quad (26)$$

where Z_1 [Eq. (14)] accounts for the near-surface acceleration and approaches the linear and constant terms of Eq. (25) as depth approaches 10 m. Parameter W_0 is the initial downward velocity at the surface. The present dataset is inadequate to determine accurately the parameters of Z_1, but a value of $W_0 = 0$ would yield empirically the offset of about −4 m found in the analysis. Further study of the near-surface transient problem is indicated. In particular, an experiment in water at least 10 m deep will be required where probes can be tracked to within a few centimeters and timed to within a few milliseconds. During this experiment, several series of probe drops should be made, varying parameters such as height above the surface, angle from the vertical, and amount of vertical rotation (i.e., "wobble"). Spinup (about probe axis) is also likely to be a factor in the overall acceleration and should be addressed.

Fig. 16. Temperature error ($T_{CTD} - T_{XBT}$) mean (solid) and standard deviation (dashed) profiles for XBT depths calculated using individually determined FREs (section 4c) and with corrected XBT temperatures.

program and provided multiple acquisition systems for the expendables. Richard Myrick of the Naval Oceanographic and Atmospheric Research Laboratory (NOARL) performed data acquisition and handled equipment logistics. Harry Meyers, Bud Stewart, and Sho Velasquez of the Naval Oceanographic Office provided valuable assistance with the operation. We are indebted to Bert Green for his many helpful suggestions. This research was funded by the Oceanographer of the Navy's (CNO OP-096) ASW Oceanography Program Office (NOARL Code 311) program elements 64704N and 63704N. The mention of commercial products or the use of company names does not in any way imply endorsement by the U.S. Navy or NOARL.

REFERENCES

Fedorov, K. N., A. I. Ginzburg, and A. G. Zatsepen, 1978: Systematic differences in isotherm depths derived from XBT and CTD data.

POLYMODE News, 50(1), 6–7. [Unpublished manuscript available through WHOI.]

Flierl, G., and A. R. Robinson, 1977: XBT measurements of thermal gradient in the MODE eddy. *J. Phys. Oceanogr.*, 7, 300–302.

Green, A. W., 1984: Bulk dynamics of the expendable bathythermograph (XBT). *Deep-Sea Res.*, 31, 415–426.

Hallock, Z. R., and W. J. Teague, 1990: XCTD test: Reliability and accuracy study (XTRAS). NOARL TN 69, 33 pp.

Hanawa, K., and H. Yoritaka, 1987: Detection of systematic errors in XBT data and their correction. *J. Oceanogr. Soc. Japan*, 43, 68–76.

Heinmiller, R. H., C. C. Ebbesmeyer, B. A. Taft, D. B. Olson, and O. P. Nikitin, 1983: Systematic errors in expendable bathythermograph (XBT) profiles. *Deep-Sea Res.*, 30, 1185–1197.

McDowell, S., 1977: A note on XBT accuracy. *POLYMODE News*, 29(1), 4–8. [Unpublished manuscript available through WHOI.]

Seaver, G. A., and S. Kuleshov, 1982: Experimental and analytical error of the expendable bathythermograph. *J. Phys. Oceanogr.*, 12, 592–600.

Singer, J. J., 1990: On the error observed in electronically digitized T-7 XBT data. *J. Atmos. Oceanic Technol.*, 7, 603–611.

Wright, D., and M. Szabados, 1989: Field evaluation of real-time XBT systems. *Oceans 89, Proc.* 5, 1621–1626.